Essentiality of the virulence plasmid-encoded factors in disease pathogenesis of the major lineage of hypervirulent *Klebsiella pneumoniae* varies in different infection niches

Carey Lim,[a,b] Chu-Yun Zhang,[a,b] Guoxiang Cheam,[a,b] Wilson H. W. Chu,[a,b,c] Yahua Chen,[a,b] Melvin Yong,[a,b] Kai Yi E. Lim,[d] Margaret M. C. Lam,[e] Teck Hui Teo,[d] and Yunn-Hwen Gan[a,b,*]

[a]Infectious Diseases Translational Research Programme, Yong Loo Lin School of Medicine, National University of Singapore, 5 Science Drive 2, MD4, Level 2, 117545, Republic of Singapore
[b]Department of Biochemistry, Yong Loo Lin School of Medicine, National University of Singapore, MD7, 8 Medical Drive, 117596, Republic of Singapore
[c]National Public Health Laboratory, National Centre for Infectious Diseases, 16 Jln Tan Tock Seng, 308442, Republic of Singapore
[d]A*STAR Infectious Diseases Labs, Agency for Science, Technology and Research, 8A Biomedical Grove #05-13, Immunos, 138648, Republic of Singapore
[e]Department of Infectious Diseases, School of Translational Medicine, Monash University, Melbourne, Victoria, 3004, Australia

eBioMedicine
2025;115: 105683
Published Online xxx
https://doi.org/10.1016/j.ebiom.2025.105683

Summary

Background Hypervirulent *Klebsiella pneumoniae* (Hv*Kp*) can metastasise to extra-intestinal sites to cause disseminated disease such as pyogenic liver abscesses. Hv*Kp* harbours a large virulence plasmid (*Kp*VP) that contributes to pathogenicity. We previously identified a crucial gene region that confers virulence in SGH10 (ST23, K1 capsule), spanning genes encoding the siderophores aerobactin and salmochelin, as well as the regulator of mucoidy phenotype A (*iuc-rmp-iro*).

Methods SGH10 isogenic mutants of aerobactin, *rmpA*, and salmochelin were generated and tested *in vitro* for their siderophore production, hypermucoviscosity and growth. We investigated the essentiality of these factors in different murine infection or colonisation models.

Findings In a lung pneumonia model, capsule modulation by *rmpA* was the primary driver of high bacterial burden in the lung. In a systemic infection setting, *rmpA* was still the primary driver, followed by a significant contribution by salmochelin, that conferred virulence. However, the role of aerobactin was more significant in hv*Kp* persistence in the gut. We further examined a large collection of *Kp* genomes and observed that the *iro* loci is often co-inherited with *iuc* in *Kp*VP-1, suggesting the evolutionary importance of expressing both siderophores in these lineages.

Interpretation Hv*Kp* typically colonises the intestinal niche, however, the acquisition of the *Kp*VP plasmid has enabled it to thrive outside the gut and cause metastatic infections. While the *iuc-rmp-iro* region is pivotal in bestowing virulence, the encoded factors contribute differently to the success of the pathogen in various infection sites, where the microenvironment, nutrient availability and immune response can vary. Thus, our study demonstrates that possessing the *iuc-rmp-iro* gene region can be an evolutionary advantage by allowing for flexibility in modulating siderophore and capsule expression in order for *K. pneumoniae* to thrive in distinct host niches.

Funding This work is funded by the National Research Foundation MOH-000925-00 to YH Gan and OFYIRG22jul-0042 by the National Medical Research Council (NMRC) to THT.

Keywords: *Klebsiella pneumoniae*; Hypervirulent; Plasmid; Liver abscess; Siderophore

*Corresponding author. Infectious Diseases Translational Research Programme, Yong Loo Lin School of Medicine, National University of Singapore, 5 Science Drive 2, MD4, Level 2, 117545, Republic of Singapore.
E-mail address: bchganyh@nus.edu.sg (Y.-H. Gan).

Research in context

Evidence before this study

Carriage of a large virulence plasmid is a known hallmark of hypervirulent *Klebsiella pneumoniae* that causes severe metastatic infections even in healthy individuals. The large virulence plasmid harbours an arsenal of virulence determinants—aerobactin, *rmpA*, and salmochelin, which collectively confer hv*Kp* an enormous survival advantage through augmented iron acquisition and immune evasion capabilities. However, the specific requirements for each of these factors in pathogenesis in the context of different *in vivo* infection sites have not been comprehensively explored.

Added value of this study

In this study, we focus on a representative hypervirulent Sequence-Type (ST) 23 K1 strain, SGH10, and delineate the specific requirements for aerobactin, *rmpA*, and salmochelin for successful establishment at various host infection sites using different mouse models. We show that the *rmp* locus is the most important factor in determining bacterial virulence in the lung infection and in systemic infection. In addition, salmochelin also contributes to virulence in a systemic infection setting, while aerobactin is important for the maintenance of stable gut colonisation. We further examined bioinformatically an extensive number of *Kp*VP-1-harbouring *Kp* strains for their carriage of *iro* and *iuc* loci and observed the common co-inheritance of *iro* with the *iuc* especially in hypervirulent lineages.

Implications of all the available evidence

It appears that the genes in the virulence plasmid *iuc-rmp-iro* region have co-evolved together to provide important adaptations that allow hv*Kp* to thrive in different host niches. Understanding the essentiality of each virulence factor for pathogenicity in different infection niches will guide the development of strategies for precision targeting of the pathogen.

Introduction

Klebsiella pneumoniae is one of the ESKAPE pathogens highlighted on the World Health Organisation's critical priority list of bacteria in dire need of novel treatments due to extensive drug resistance. In 2019, *K. pneumoniae* was responsible for over 200,000 deaths attributed to antimicrobial resistance (AMR), making it the second leading bacterial cause of mortality.[1] Particularly concerning are the reports from Asia on the convergence of hypervirulence and multi-drug resistance (MDR) in *K. pneumoniae* in the past decade. These convergent strains exhibit both virulence traits associated with hypervirulent lineages of *K. pneumoniae* while also harbouring MDR genes, particularly against the drug of last resort, carbapenem, making these "superbug" strains a harbinger of a global healthcare crisis. This convergence occurs through two major mechanisms: hypervirulent *K. pneumoniae* (hv*Kp*) strains acquiring the AMR genes or plasmids such as ST23-blaKPC and ST65-blaCTX-M[2] in China and Singapore[3] or MDR classical *K. pneumoniae* strains acquiring the virulence plasmid observed in ST11-blaKPC in China,[4] ST231-blaOXA-232 in India.[5]

Hv*Kp* are often community-acquired and can inhabit different host niches depending on the stage of infection. In many cases, these strains can colonise the intestinal tracts of carriers without causing disease.[6] In certain individuals, hv*Kp* may be able to translocate across the intestinal epithelium and metastasise to other parts of the body, often targeting the liver, lungs, spleen, meninges, and eyes.[7] Hv*Kp* are typically characterised by the presence of the regulator for mucoid phenotype (*rmpA*) gene locus as well as salmochelin and aerobactin siderophores. The major hv*Kp* lineages belong to ST23, ST86, and ST65, which all carry a large virulence plasmid containing the *rmp*, aerobactin, and salmochelin operons.[8,9] Several studies have highlighted the importance of *Kp*VP during systemic infection.[10,11] Some studies have also examined the contribution of individual genetic determinants such as *rmpA* or aerobactin during hv*Kp* infection. However, due to the diverse genetic makeup of *K. pneumoniae* strains and the use of different models, it is challenging to reach a consensus on which elements on the *Kp*VP are critical for bacterial pathogenesis. A recent study compared the contribution of the virulence plasmid of seven strains from different ST lineages and found that while the contribution of the virulence determinants, such as *rmpA*, on the virulence plasmid was generally conserved across the strains, the contribution of iron siderophores varied.[12]

To counter the spread of virulence determinants into MDR or carbapenem-resistant strains, or the acquisition of MDR plasmids into hypervirulent strains, we require a comprehensive understanding of the role of each virulence determinant during disease pathogenesis. Bacterial adaptation and virulence are heavily influenced by modes of exposure and infection routes. Therefore, we hypothesise that ascertaining the relative importance of each genetic element on the *Kp*VP to disease pathogenesis in a context-dependent manner will be critical for designing precise targeting strategies against the bacteria. To achieve this, we selected the canonical ST23 K1 capsular type strain SGH10 isolated from a patient with liver abscess[9] to represent the hv*Kp* lineage, which is responsible for causing the majority of pyogenic *Klebsiella*-liver abscess cases. Our findings demonstrate that the contribution of each virulence factor to the overall pathogenesis of the bacteria greatly

depends on the organ niche, demonstrated through different routes of infection. This allows us to more accurately discern the extent of bacterial reliance on genes and genetic circuits necessary for their successful survival or proliferation in various host niches. This will, in turn, inform the development of more precise targeting strategies against the pathogen.

Methods

Bacterial strains and culture

K. pneumoniae SGH10 (Accession no.: CP025080) and its isogenic mutants were grown on Lysogeny Broth (LB) agar and in LB broth. For inoculation into mice, bacterial counts were determined by OD_{600} measurement and strains were diluted in PBS accordingly in each infection method.

Construction of SGH10 isogenic mutants and complemented strains

Gene deletion in SGH10 was performed as previously described.[13] In brief, Phanta Flash DNA Polymerase (Vazyme) amplified upstream and downstream regions of the target gene were assembled with pR6KmobsacB using NEBuilder® HiFi DNA Assembly Master Mix (New England Biolabs) and then introduced into SGH10 through conjugation using *Escherichia coli* S17 as a donor. Selection was performed with 100 μg/mL kanamycin (Sigma–Aldrich, #K1377) and 40 μg/mL fosfomycin (Sigma–Aldrich, #P5396). Negative selection was performed by overnight culturing in LB with 20% sucrose and then spreading on to LB agar plates. Viable colonies were screened using PCR and followed by nucleotide sequencing (1st Base) to validate gene deletion.

Gene complementation in SGH10 was performed with Phanta Flash DNA Polymerase (Vazyme) to amplify target gene and pACYC derivatives (Cm^R or Km^R). The genes were cloned into vectors using NEBuilder® HiFi DNA Assembly Master Mix (New England Biolabs) in *E. coli* DH5α. The DH5α containing plasmids with complement fragment was selected with 50 μg/mL chloramphenicol (Sigma–Aldrich, #AC1919) or 50 μg/mL kanamycin and then miniprepped with Monarch® Plasmid Miniprep Kit (New England Biolabs). The complementation plasmids were introduced into corresponding SGH10 deletion mutants through electroporation.

Selection was performed with 50 μg/mL chloramphenicol or 50 μg/mL kanamycin and 40 μg/mL fosfomycin. Viable colonies were screened using PCR and followed by nucleotide sequencing to validate gene deletion. The empty vector backbone pACYC184Δ*tet* was introduced into SGH10 wild-type, Δ*iroB* and Δ*iucCD* mutants as controls.

A list of primers that were used and their sequences can be found in Table 1, while isogenic mutants used in this study are listed in Table 2.

Primer name	Sequence
entB Up-for	ccaagcttgcatgcctgcagGCGGCTACTACAACAGCC
entB Up-rev	agcgccgccaTCTCTGTTCTCCTTCAGCC
entB Dn-for	agaacagagaTGGCGGCGCTGGATTTTC
entB Dn-rev	tatgacatgattacgaattcCGGTCAGCGCCAGGCTTT
ybtS Up-for	ccaagcttgcatgcctgcagCGCTGTTCAGCGGCGGCA
ybtS Up-rev	acagttactcCCCTTACCTCTCTGTGTTATTCCCGG
ybtS Dn-for	gaggtaagggGAGTAACTGTTTTCTAACCTC
ybtS Dn-rev	tatgacatgattacgaattcGTGTGAAAACACGGTCAATAAG
iroB complement-for	cgcagtcaggcaccgtgtatGTGCGTATTCTCTTTATTGG
iroB complement-rev	gaggtgccgccggcttccatTTATTGCCAGATGGTTTTC
iucCD complement-for	catgattacgaattcTTCACGGAGGTCGGTCTGTA
IucABCD complement-for	catgattacgaattcgctctcaagagacgtcacga
iucCD/*iucABCD* complement-rev	cttgcatgcctgcagcagcccaaagatgctgtgta

Table 1: **List of primers used for cloning and mutant generation.**

Chrome azurol S (CAS) assay for quantification of siderophore activity

The CAS assay was performed following a previously described protocol[10,15] with several modifications. 2 mM CAS (Sigma–Aldrich, #C1018) dissolved in 50 mL distilled water was mixed with 9 mL of 1 mM ferric chloride ($FeCl_3 \cdot 6H_2O$; Sigma–Aldrich, #157740) solution in 10 mM HCl. This mixture was then added to 40 mL of 5 mM Cetyltrimethylammonium bromide (CTAB) (Sigma Aldrich, #H6269) in distilled water. The blue-colour CAS-CTAB solution was sterilised with 0.22 μM filter before use and diluted with sterile water.

Mutations	Description	Reference
SGH10 wild-type	K1 CG23-I KLA isolate	9,14
SGH10 Δ*KpVP*	SGH10 large virulence plasmid *KpVP* cured mutant	10
SGH10 Δ*rmpA*	SGH10 with no hypermucoid capsule production	13
SGH10 Δ*wcaJ*	SGH10 capsule-null mutant	13
SGH10 Δ*iuc-rmp-iro*	SGH10 *KpVP* partial deleted region comprising of aerobactin, *rmp* operon and salmochelin	10
SGH10 Δ*iucCD*	SGH10 with impaired aerobactin synthesis	10
SGH10 Δ*iroB*	SGH10 with no salmochelin glycosyltransferase on *KpVP*	10
SGH10 Δ*iroBiucCD*	SGH10 double mutant lacking salmochelin glycosyltransferase and aerobactin synthesis on *KpVP*	This study
SGH10 Δ*iroN*	SGH10 with no salmochelin outer membrane receptor	10
SGH10 Δ*ybtS*	SGH10 with impaired yersiniabactin synthesis	This study
SGH10 Δ*entB*	SGH10 with impaired enterobactin synthesis	This study
SGH10 Δ*iroB*/pACYC:*iroB*	SGH10 Δ*iroB* mutant with *iroB* complemented on pACYC plasmid	This study
SGH10 Δ*iroB*/pACYCΔ*tet*	SGH10 Δ*iroB* mutant with empty pACYC plasmid	This study
SGH10Δ*iucCD*/pACYCΔ*tet*	SGH10 Δ*iucCD* mutant with empty pACYC plasmid	This study
SGH10Δ*iucCD*/pACYC:*iucCD*	SGH10 Δ*iucCD* mutant with *iucCD* complemented on pACYC plasmid	This study
SGH10Δ*iucCD*/pACYC:*iucABCD*	SGH10 Δ*iucCD* mutant with *iucABCD* complemented on pACYC plasmid	This study

Table 2: **SGH10 and its isogenic mutants.**

Overnight bacterial cultures grown in DMEM (Cytiva, SH30243.01) with 10% FBS (Cytiva, #SH30070.03), 2-(N-morpholino) ethanesulfonic acid (MES)-buffered DMEM with 10% FBS (pH = 7), iron chelated (200 μM 2-2′Bipyridyl (BIP, MP Biomedicals, #01614)) DMEM with 10% FBS or 25% mouse serum were diluted to 10^8 CFU in 1 mL in the respective media and incubated for 24 h at 37 °C with shaking. Samples were centrifuged at 3000 g for 10 min and 100 μL of supernatant was mixed with 100 μL of CAS-CTAB reagent in a 96-well flat bottom clear plate, while the same volume of media was used as control. A minimum of 3 biological repeats were performed. The plate was incubated for 1 h at 37 °C. Absorbance at OD_{630} was measured and percentage siderophore units (psu) was calculated using the following formula:

$$\frac{(OD_{630}Media - OD_{630}Sample)}{OD_{630}Media} \times 100\%$$

Hypermucoviscosity assay

To quantify hypermucoviscosity levels, each strain was grown overnight in LB or DMEM supplemented with 10% FBS, then diluted to 10^9 CFU in 1 mL in an Eppendorf tube in the respective media. Strains were then centrifuged at 1000 g for 5 min and supernatants transferred into 96-well plates for OD_{600} reading in triplicate. Capsule-null Δ*wcaJ* strain was used as a negative control.

Mouse infection models

Female C57BL/6 mice aged between 7 and 10 weeks purchased from InVivos were used for all experiments. All mice were maintained in a murine pathogen–free animal biosafety level-2 facility at National University of Singapore in compliance with National Advisory Committee for Laboratory Animal Research (NACLAR) guidelines and acclimatized for 3 days. For intranasal administration, mice are anaesthetised in an isofluorane chamber and inoculated intranasally with 60 μL of PBS containing 10^2–10^3 CFU of wild-type SGH10 and its respective isogenic mutants. For intraperitoneal infection, mice were restrained, and the injection site sterilised with ethanol. Strains were diluted to 10^3–10^6 CFU in 100 μL PBS and injected using a 27G needle. For survival experiments, mice were monitored twice daily and were euthanised upon assessment of humane endpoint (weight loss of more than 20% body weight).

CFU enumeration of organ bacterial loads

At the appropriate timepoints, mice were euthanised by CO_2. Blood from mice was freshly collected from the vena cava into Eppendorf tubes containing 10 μL of 0.5 M EDTA to prevent coagulation, serially diluted and plated for enumeration. Liver, lungs, and spleen were collected into pre-weighed bead tubes containing PBS (OMNI, #19-768, #19-627), homogenised, serially diluted and plated for enumeration. LB plates supplemented with 100 μg/mL carbenicillin (Sigma Aldrich, #C1389) were used for selection of *K. pneumoniae*. Lung tissues were processed as described.[16] Briefly, lungs were pre-weighed and homogenised in 2 mL of LB supplemented with carbenicillin. Tissue lysates were centrifuged at 300 g for 5 min and *K. pneumoniae* loads were enumerated by serial dilution of supernatants. For all cases, the limit of detection of recovered colonies differs for each sample due to varying collected sample weights. Therefore, where no colonies were enumerated, data was plotted as 1 for the purposes of presentation on a log axis. This is also applicable to stool CFU enumeration as described in the next section.

Gut colonisation model

Mice were pre-administered with 2.5 mg ampicillin (Sigma–Aldrich, #A9518) daily via oral gavage for three consecutive days. Overnight cultures of SGH10 and its mutants were then diluted to 10^6 CFU and inoculated into mice via oral gavage in 100 μL PBS. Stool pellets were collected in PBS from mice at each timepoint during colonisation, weighed, homogenised and vortexed for 2 min at high speed to break down stool pellets into slurry. Stool slurry was serially diluted and plated on LB agar supplemented with 100 μg/mL carbenicillin to enumerate colonisation loads.

Collection of mouse serum and caecal filtrate

Mice were euthanised with CO_2 and blood was immediately drawn from the vena cava using a 27G needle. Blood was allowed to coagulate at room temperature for 30 min and then centrifuged at 4 °C at 8000 rpm for 10 min. Serum was collected and stored immediately at –80 °C. Caecum was harvested from naive mice and dissected to collect caecal content into a pre-weighed Eppendorf tube. Caecal content was diluted in five volumes of PBS and vortexed for two minutes. Caecal content was then centrifuged at 16,000 g for eight minutes and supernatant passed through a 0.22 μM filter.

Enzyme-linked immunoabsorbent assay (ELISA)

The concentration of lipocalin-2 (LCN2) in stool slurry was detected using ELISA. During each colonisation timepoint, stools were collected in PBS, homogenised and vortexed for two minutes. Stool slurries were centrifuged at 16,000 g for 8 min and supernatant collected and stored at –80 °C before usage. Slurries were diluted two-fold in assay buffer for sandwich ELISA assay which was carried out according to the manufacturer's instructions (R&D Systems, DY1857).

Growth assay

Overnight culture of each strain was diluted 2000-fold into fresh LB, M9 minimal media supplemented with 20% glucose, 50% caecal media, 25% mouse serum or

DMEM supplemented with 10% FBS. OD_{600} was recorded on a Tecan Infinite® M Plex microplate reader every 30 min for 24 h at 37 °C and used to generate growth curves.

In vitro evolution of SGH10

SGH10 was grown overnight in LB and subcultured daily by inoculating 4.88 µL of the culture into 5 mL of fresh LB, corresponding to an approximate 10-generation increment per subculture. The cultures were propagated for a total of 300 generations. Single colonies were subsequently isolated for Oxford Nanopore sequencing. The raw sequencing files were deposited to NCBI Sequence Read Archive Database under Bioproject accession number PRJNA801425.

Screening of *iuc* and *iro* loci in *K. pneumoniae* genomes

Presence of *iuc* and/or *iro* loci associated with the *Kp*VP-1 virulence plasmid (i.e., *iuc 1* and *iro 1* lineages) was examined in a public collection of 47,721 *K. pneumoniae* genomes available on Pathogenwatch (https://pathogen.watch/)[17] as of October 2024. Genotyping of these genomes had been performed with Kleborate (version 2.3.0),[18] and the output was used to examine the presence of *iuc1* and/or *iro1* (reported in the 'Aerobactin' and 'Salmochelin' columns of the Kleborate output, respectively). Sublineages had been defined using 629-loci core genome MLST (cgMLST) and associated 'cgLIN' (Life Identification Number) code nomenclature.[19] Data exploration and visualisation was performed using ggplot2 in R, and the final figure was plotted using the geom_point function.

Statistics

Statistical analysis was performed using GraphPad Prism 7. Ordinary one-way ANOVA with multiple comparisons was used to analyse siderophore quantitation and hypermucoviscosity data. Kaplan–Meier survival curve with Gehan-Breslow-Wilcoxon method was used to compare mouse survival results between wild-type and mutants. Kruskal–Wallis multiple comparisons test was used to compare organ CFUs enumerated between wild-type SGH10 and its mutants from infected organs and intestinal colonisation. Two-way ANOVA with Dunnett's multiple comparison test was used to compare gut colonisation loads over 14 days wild-type SGH10 and its mutants. To calculate LD_{50}, the probability of mortality was modelled against the Log_{10} transformed infection dose. Then, the models were fitted in R using the logistic regression model from the default 'stats' package. Parameters (β_0 and β_1) of the logistic model were used to calculate the LD_{50} values. Area under the curve (AUC) was generated for each mouse in each group during gut colonisation after Log_{10} transformation of CFU data from 5 to 14 dpi. Data was then analysed by Kruskal–Wallis multiple comparisons test.

Ethics statement

Mouse experiments involving intraperitoneal administration and gut colonisation were reviewed and approved (Protocol no: R21-1498) by National University of Singapore Institutional Animal Care and Use Committee (NUS IACUC) under rules and regulation of the National Advisory Committee for Laboratory Animal Research (NACLAR). Mouse intranasal infection was carried out at A*STAR Biological Resource Centre and approved by A*STAR IACUC under NACLAR guidelines (Protocol no: 231754).

Role of funders

The funders had no role in the decision to publish or the preparation of this manuscript.

Results

Siderophore production and hypermucoviscosity

In our previous work, we described the *Kp*VP plasmid-cured SGH10 and demonstrated its contribution to virulence in a systemic infection model.[10] In this study, we utilised isogenic deletion mutants in *rmpA* and in the aerobactin (Δ*iucCD*) and salmochelin (Δ*iroB*) synthetic clusters, as well as a double siderophore mutant (Δ*iroBiucCD*) to functionally characterise the role of these individual virulence determinants.

We measured the siderophore production of wild-type and mutants in both cell culture media (DMEM + 10% FBS) and mouse serum. For comparison, we also included deletion mutants of two chromosomally encoded siderophores - enterobactin (Δ*entB*) as well as yersiniabactin (Δ*ybtS*), where the latter is situated on an integrative conjugative element ICE*Kp*10 in SGH10. As our siderophore quantification assays were done on bacteria cultured overnight, the acidic medium conditions contributed by bacterial growth could favour aerobactin production.[20] Hence, we also cultured bacteria in pH-buffered DMEM (pH 7). Our results demonstrated that in both cell culture media, deletion of aerobactin (Δ*iucCD*) consistently resulted in a decrease in siderophore production (Fig. 1a and b), whereas complementation of the *iuc* genes rescued this phenotype (Supp Fig S1a). We also consistently see a significant decrease in siderophore production in the Δ*entB* mutant. Under iron-limiting conditions with the addition of an iron chelator, the Δ*entB* mutant had the most significant drop in siderophore production followed by the Δ*iucCD* and Δ*iroBiucCD* double mutant. This suggests that enterobactin and aerobactin comprise the largest proportion of the siderophore pool produced by SGH10 under iron limitation or was the most efficient in chelating iron in the CAS assay (Fig. 1c). There were no changes with deletion of other siderophores, likely indicating that all siderophores were made maximally and reached saturation compared to wild-type, so they were redundant in the assay. In mouse serum, which

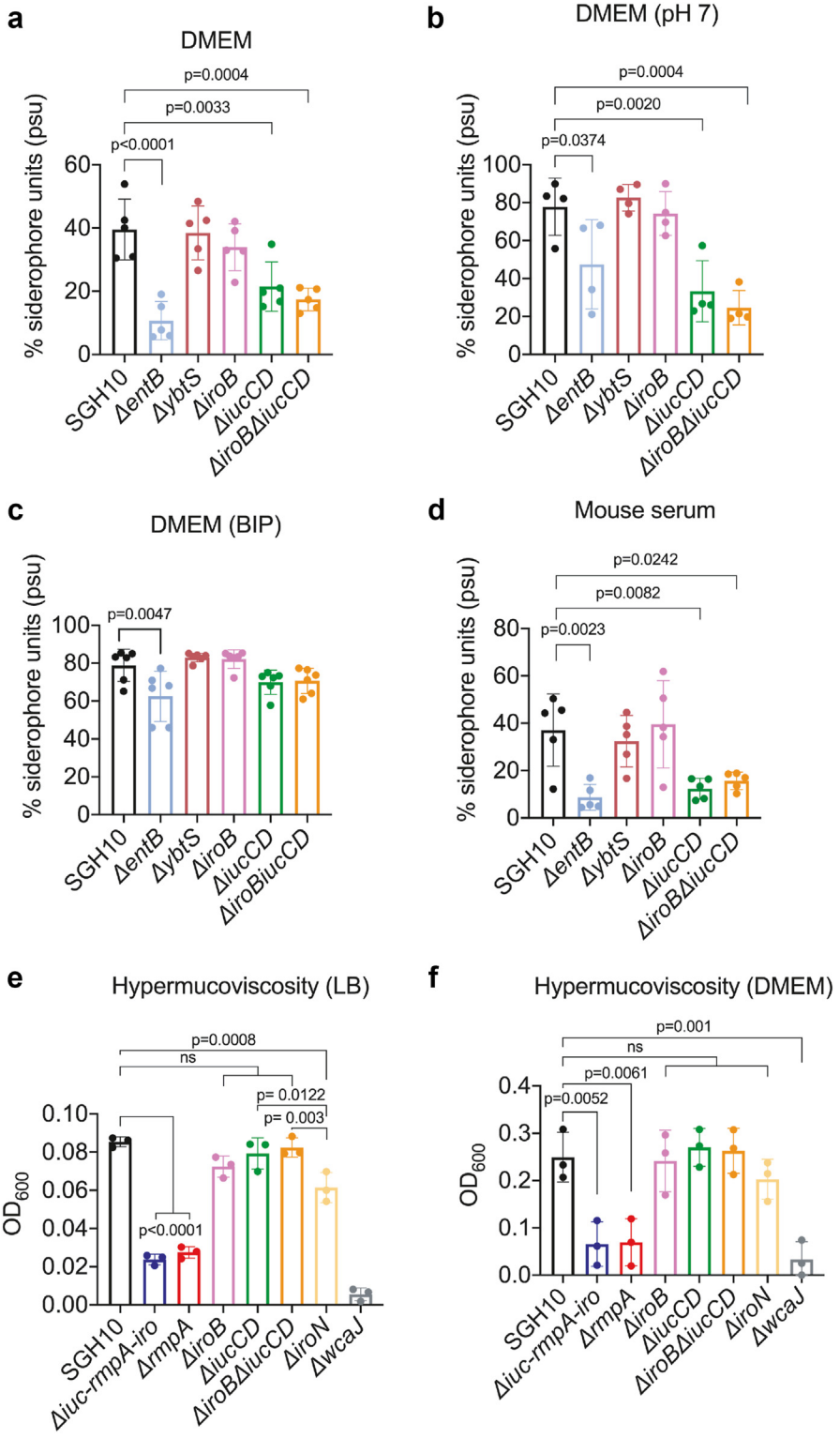

Fig. 1: **SGH10 predominantly produces aerobactin, enterobactin, and enterobactin-derived siderophores**. Siderophore quantification of SGH10 and its mutants cultured in **a)** DMEM + 10% FBS, **b)** MES-buffered DMEM (maintained at pH 7), **c)** DMEM supplemented with 200 uM 2-2′Bipyridyl (BIP) and **d)** 25% mouse serum. Hypermucoviscosity quantification for SGH10 and mutants cultured overnight in **e)** LB media or **f)** DMEM + 10% FBS with capsule-null Δ*wcaJ* as a negative control. Data was analysed by one-way ANOVA. Bar graphs represent Mean ± SD, each dot represents one biological replicate.

would likely more closely resemble the environment during systemic spread, enterobactin deletion resulted in the most severe drop in siderophore production, followed by aerobactin deletion (Fig. 1d).

This aligns with observations in other hypervirulent strains that found aerobactin to be the primary siderophore needed for growth in human urine, serum or ascites fluid.[21] Additional deletion of salmochelin (Δ*iroBiucCD*) did not result in a further reduction of total siderophores (Fig. 1a–d). However, given that *iroB* encodes the C-glucosyltransferase that glucosylates enterobactin to yield salmochelin,[22] disrupting this biosynthetic step may not affect total siderophore levels as the enterobactin substrate would still be present. Since deletion of enterobactin significantly reduced siderophore levels, it suggests that both enterobactin and enterobactin-derived siderophores (such as salmochelin) could contribute substantially to total siderophore production in SGH10.

Hypermucoviscosity has been reported to be modulated by iron.[23,24] Therefore, we also measured and compared hypermucoviscosity among the mutants. We included the capsule null mutant Δ*wcaJ* as our negative control and the Δ*iroN* mutant as it would be used later for mouse survival studies. Our findings showed that compared to wild-type SGH10, deletion of aerobactin or salmochelin did not significantly alter hypermucoviscosity in either LB (Fig. 1e) or DMEM (Fig. 1f). However, the deletion of *iroN*, a receptor for salmochelin, did lead to a marginal reduction in hypermucoviscosity. We also analysed the growth kinetics of these mutants in various culture conditions and found no apparent fitness defect despite the loss of siderophore production or *rmpA* (Supp Fig S2a–d).

Essentiality of virulence plasmid's *rmpA* and not siderophores during lung infection

Disseminated hv*Kp* often colonise the lungs, leading to acute pulmonary infection and pneumonia.[25] To investigate the importance of the major virulence factors on the *Kp*VP plasmid for replication in the lungs, we tested the different SGH10 isogenic mutants in the pneumonia model. In this model, mice are inoculated intranasally with a low dose of *K. pneumoniae* (10^3 CFU) that reaches the deeper part of the lungs where early bacterial replication in the lungs progresses to disseminated infection and sepsis.

Lung bacterial burdens were enumerated at 48 h post infection (hpi), showing that the regulation of hypermucoviscosity and capsule production by *rmpA* was the primary driver of virulence in the lung, as deletion of *rmpA* alone was able to severely restrict the establishment of SGH10 (Fig. 2a). Conversely, the aerobactin and salmochelin mutants alone or in combination failed to attenuate bacterial growth in the lungs (Fig. 2a). Concordant with the lung bacterial load profile, loss of hypermucoviscosity in Δ*rmpA*-infected mice rescued mice from mortality at a 10^3 CFU infection dose (Fig. 2b). Interestingly, while there was no effect of aerobactin alone (Δ*iucCD*) nor any statistical significance with salmochelin mutant (Δ*iroB*), the Δ*iroBiucCD* double mutant showed significant alleviation in mortality (Fig. 2b). However, the greatest attenuation was still due to loss of *rmpA*.

To understand whether the role of the virulence plasmid determinants is dose dependent in this lung infection model, we lowered the infection dose to 10^2 CFUs. At this infection dose, even the wild-type strain had poor establishment of infection (~60% infection) (Fig. 2c). Interestingly, the lung bacterial burden appeared higher in Δ*iroB* and Δ*iroBiucCD* double mutant, but did not reach statistical significance because of the smaller sample size. Altogether, hypermucoviscosity conferred by *rmpA* played the major role in virulence in the pulmonary infection model.

Significance of *rmpA* and salmochelin during systemic infection

The delayed mortality in salmochelin mutant-infected mice in the lung models despite similar or higher acute lung burden could reflect the importance of salmochelin during dissemination. Mice were infected intraperitoneally to model systemic infection where hv*Kp* disseminates through the blood and seed distal organs such as the lungs. While we had previously shown that loss of *Kp*VP completely abrogates the virulence of SGH10 in systemic infection,[10] we now further demonstrate that deletion of the *iuc-rmp-iro* region is sufficient to attenuate virulence to the same extent as the *Kp*VP null mutant even with a high dose of infection at 10^6 CFU (Fig. 3a). With a 10-fold titration in infectious dose, the data indicate that Δ*iroB* and Δ*iroBiucCD* mutants might be attenuated at 10^5 CFU although the dose was still too lethal to observe a distinct difference from wild-type (Fig. 3b). The clearest differentiation between the various mutants from wild-type infection was at a dose of 10^4 CFU where the Δ*iucCD* mutant was still as virulent as wild-type but Δ*iroB* was significantly attenuated (Fig. 3c). The Δ*rmpA* mutant was highly attenuated but less than the *iuc-rmpA-iro* region deletion mutant, which was completely attenuated. At 10^3 CFU, there was no differentiation between Δ*rmpA* and the *iuc-rmpA-iro* deletion mutant, and the attenuation of Δ*iroB* was still present while Δ*iucCD* did not reach statistical significance (Fig. 3d). The calculated LD_{50} values also rank the order of virulence from highest LD50 values as: *iuc-rmpA-iro, rmpA, iroBiucCD, iroB, iucCD,* and wildtype (Supp Fig S1b). Thus, we demonstrate that while *rmpA* is the most dominant virulence factor in systemic infection, salmochelin also contributes to virulence, whereas the loss of aerobactin has a small impact. Supporting this conclusion, deletion of *iroN*, which prevents the bacteria from taking up iron-bound salmochelin, similarly reduced mortality

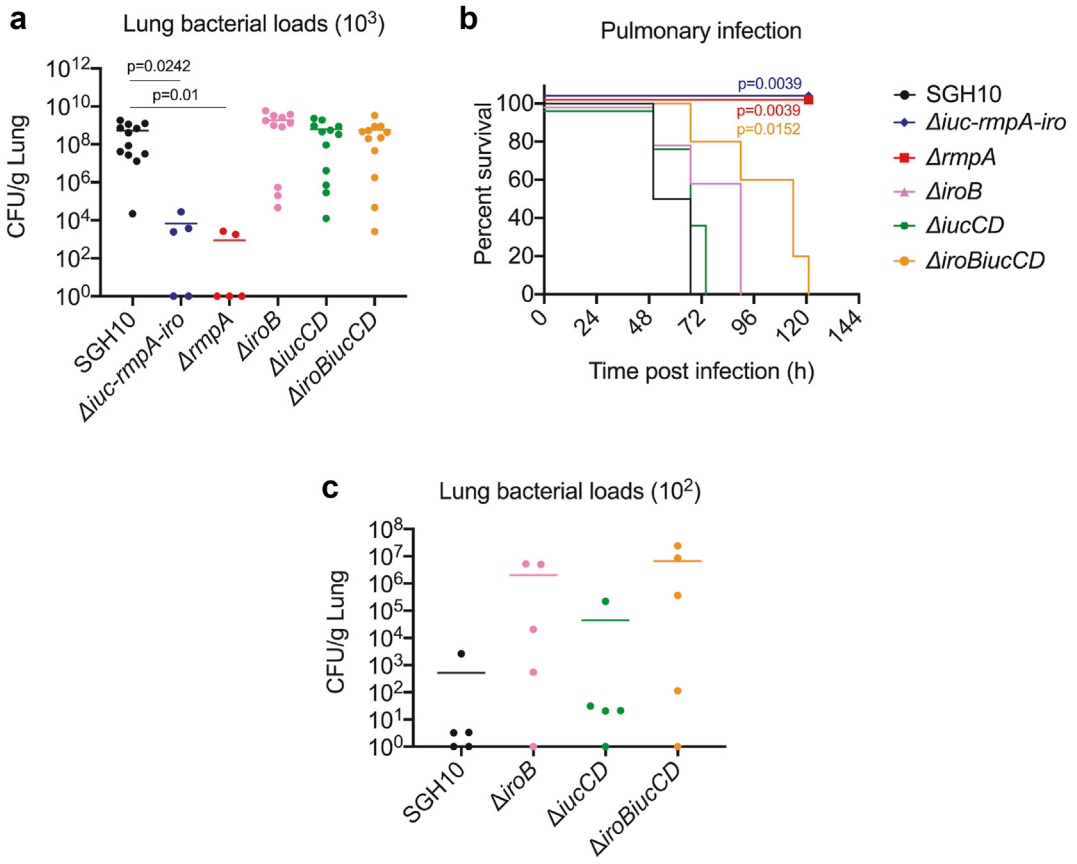

***Fig. 2: rmpA* is responsible for bacterial growth in the pneumonia model**. **a)** CFU burden in the lungs were enumerated at 48 hpi following intranasal administration with 10^3 of SGH10 and its mutants. **b)** Kaplan–Meier survival curve of mice infected via intranasal administration with 10^3 CFU of SGH10 and its mutants. **c)** CFU burden in lungs of mice at 48 hpi following intranasal administration with 10^2 CFU of SGH10 and its mutants. Where no colony was enumerated at the limit of detection, data was plotted as 1 on log axis. Means are represented. Data was analysed by Kruskal–Wallis test. Each dot represents one mouse. Statistical comparison was performed by Gehan-Breslow-Wilcoxon test between wild-type and each mutant. Data comprises n = 4–5 mice per group.

(Fig. 3c), validating the importance of salmochelin-mediated iron acquisition in systemic virulence of SGH10.

We next performed bacterial load quantification in the blood (Fig. 3e), spleen (Fig. 3f), lungs (Fig. 3g), and liver (Fig. 3h) to further understand the importance of each virulence factor during bacterial dissemination. Since the impact on mortality between the different mutants was most differentiated at the 10^4 CFU infection dose, bacterial loads were only enumerated at this dose at 12hpi. Supporting the role of salmochelin in systemic virulence, we observed a partial reduction in bacterial load in the blood, spleen, lungs and liver of Δ*iroB* infected mice (Fig. 3e–h). A similar degree of bacterial load reduction was observed in Δ*rmpA* infected mice. Complementation of *iroB* in the mutant also appeared to rescue the drop in organ bacterial loads (Supp Fig S1c). Together, the data support that *rmpA* is the most critical virulence factor in mediating disseminated hv*Kp* infection, followed by salmochelin, and less so by aerobactin.

Importance of *rmpA* and iron siderophores for gut colonisation

The use of antibiotic pre-treatment can disrupt the gut microbiota, creating a permissive environment for SGH10 colonisation. When mice were colonised through oral gavage with bacteria cured of the large virulence plasmid Δ*Kp*VP, they maintained a much higher colonisation load over 14 days compared to mice colonised with wild-type SGH10, which typically exhibit a decrease in colonisation load starting at day five (Fig. 4a). Maintenance of the large plasmid *Kp*VP could incur significant fitness costs and affect growth. Hence, we used isogenic deletion mutants to examine the role of *rmpA*, salmochelin, and aerobactin in intestinal colonisation. In the first three days, we observed no differences in colonisation between the wild-type and its

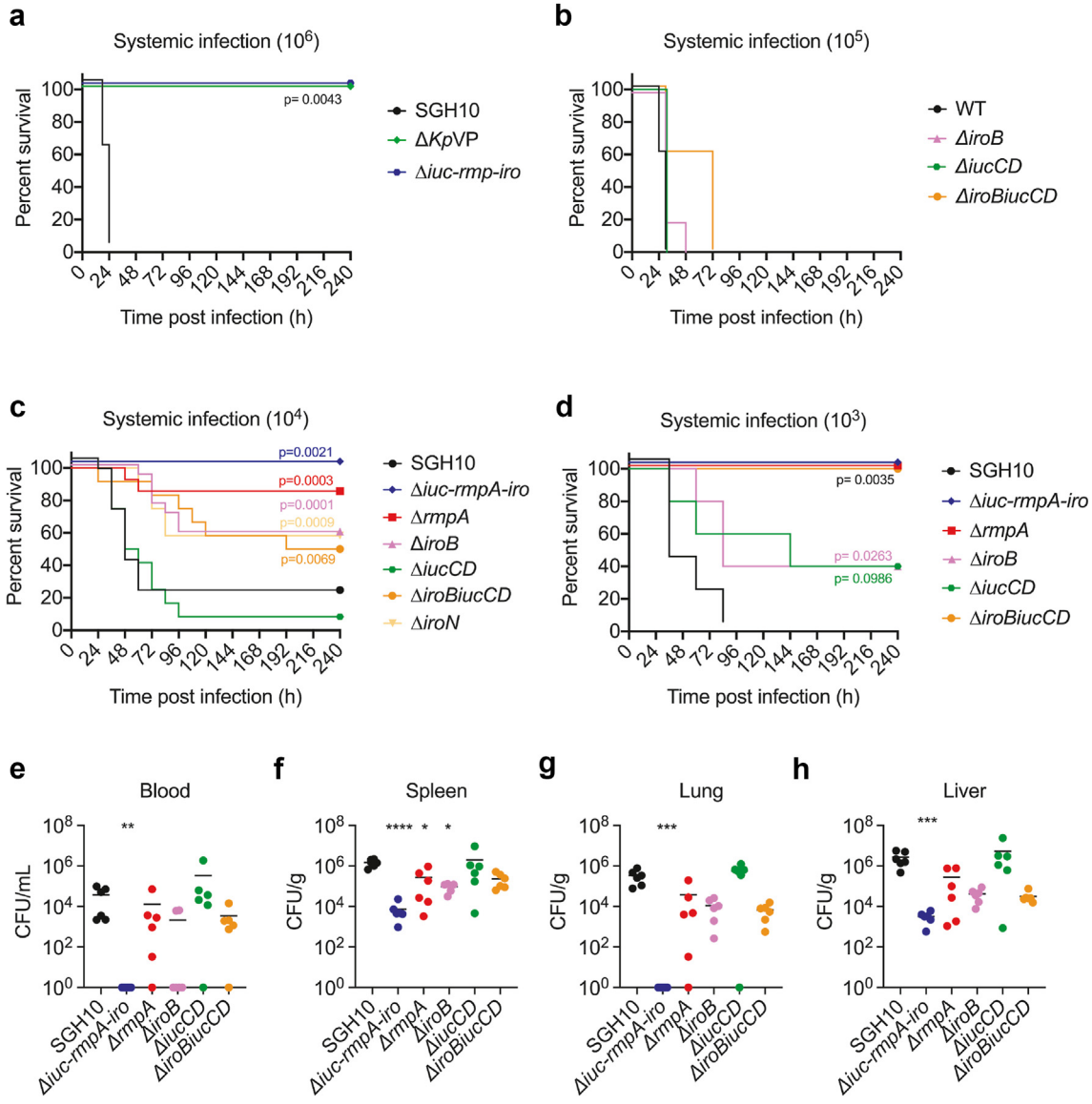

***Fig. 3: rmpA* and salmochelin contribute to virulence in systemic infection. a–d)** Mice were infected via intraperitoneal injection with 10^3–10^6 CFU of SGH10 and its mutants. Kaplan–Meier survival curves were plotted, and statistical comparison was performed by Gehan-Breslow-Wilcoxon test between wild-type and each mutant. Experiments were conducted with n = 5–16 mice per group. **e–h)** Mice were infected via intraperitoneal injection with 10^4 CFU of SGH10 and its mutants, and CFU burden in the blood, spleen, lungs and liver were enumerated at 12 hpi. Where no colony was enumerated at the limit of detection, data was plotted as 1 on log axis. Data was analysed by Kruskal–Wallis multiple comparisons test. Each dot represents one mouse, data was pooled from n = 2 experiments. Means are represented. *p < 0.05; **p < 0.01; ***p < 0.01; ****p < 0.0001.

mutants. However, as wild-type SGH10 colonisation began to drop from day five onwards, we observed a divergence in stool bacterial loads between the mutants. While the Δ*iroB* mutant demonstrated an apparent decrease in loads compared to the wild-type, the most significant decrease was observed with the Δ*iucCD* and Δ*iroBiucCD* mutants from days 5 to 14 (Fig. 4b and c). We also observed a slight reduction in growth in the Δ*iroB*, Δ*iucCD*, and Δ*iroBiucCD* mutants in caecal media (Supp Fig S2e), although it may not fully represent the *in vivo* intestinal space. Overall, it seems that aerobactin plays a more important role than salmochelin during gut colonisation.

We had previously shown that the endogenous microbiome is initially eliminated by antibiotic treatment and begins to recover from around five days of cessation.[26,27] Furthermore, it has been suggested that in germ-free mice, iron supply is sufficient in the gut as

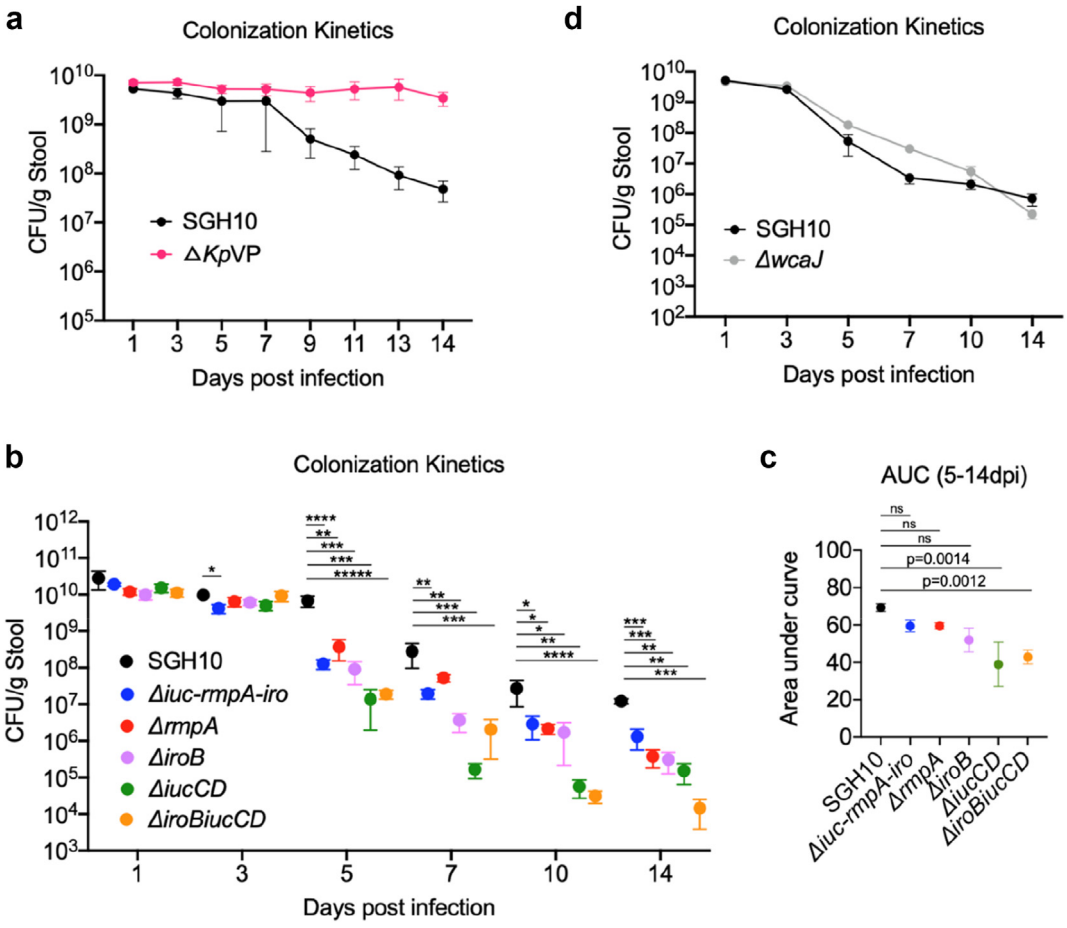

Fig. 4: **Aerobactin is pivotal for long term gut colonisation by SGH10**. Mice were pre-treated with ampicillin for three days prior to colonisation with SGH10 and its isogenic mutants by oral gavage. CFU counts were enumerated from shed stool pellets to track colonisation loads of SGH10 against its **a)** *Kp*VP-cured mutant (n = 5 mice) and **b)** its *Kp*VP gene mutants (n = 4–5 mice). **c)** Gut colonisation CFU data from **b** were Log_{10} transformed and area under the curve (AUC) calculated for SGH10 and its mutants between 5 and 14 dpi for each mouse. Data from 1 to 3 dpi was excluded due to the high colonisation loads consistent among all strains that would skew the total area calculation and make differences at later timepoints indistinguishable as colonisation loads decrease. **d)** Gut colonisation loads of mice colonised with SGH10 and its capsule-null Δ*wcaJ* mutant (n = 4–5 mice). Data in **a**, **b**, and **d** are represented by geometric mean ± SD. Data in **b** was analysed with 2-way ANOVA and Dunnett's multiple comparison test. *p < 0.05; **p < 0.01; ***p < 0.001; ****p < 0.0001. Data in **c** was analysed by Kruskal–Wallis multiple comparisons test, Mean ± SD are represented.

iron uptake genes in a colonising pathobiont were downregulated.[28] Taken together, this could mean that the differences between gut loads of wild-type bacteria and the mutants diverge due to intense competition between SGH10 and the microbiota for iron acquisition.

In addition, LCN-2 levels were elevated in the gut during SGH10 colonisation (Supp Fig S3), where it functions to sequester enterobactin that is utilised for iron acquisition by commensal bacteria such as *E. coli*.[29] In this situation, SGH10 harbouring salmochelin and aerobactin would possess a growth advantage and be able to maintain higher colonisation levels. We also noted that the *rmpA* mutant has a marginal defect in colonisation. On the contrary, the Δ*wcaJ* capsule-null mutant of SGH10 was able to colonise just as well as the wild-type (Fig. 4d). It is plausible that the fitness cost of producing capsule outweighs any potential benefit of *rmpA*-mediated increased capsule expression and hypermucoviscosity in the context of gut colonisation or microbial competition. While the *Kp*VP-cured strain can thrive in the gut, the Δ*iuc-rmp-iro* mutant does not reflect the same increased fitness but instead colonised at close to wild-type levels. There likely exists a delicate balance between the fitness cost of carrying a large virulence plasmid, versus the growth benefit of carrying siderophore genes, that determines the success of SGH10 in persisting in the highly competitive intestinal niche.

Iro locus is often co-inherited with *iuc* in KpVP1-carrying *K. pneumoniae* strains

We have so far demonstrated that the *iuc-rmpA-iro* region of *Kp*VP-1 carried by SGH10 is important to the success of SGH10 in mouse models of infection and colonisation. Interestingly, the relative contribution of the *iro* and *iuc*-encoded siderophores seems to differ by infectious niche, suggesting that harbouring both siderophores may provide a significant advantage for adaptability in different niches, both in initial colonisation of the gut and subsequent extra-intestinal infection.

We postulated that the co-inheritance of *iro* and *iuc* would confer an evolutionary advantage, and successful hypervirulent lineages bearing *Kp*VP-1 would therefore retain both loci. We thus examined nearly 4000 *K. pneumoniae* genomes that harbour the *Kp*VP-1 plasmid for their carriage of the *iro* and *iuc* loci (n = 3928/47,721 *K. pneumoniae* genomes with *iuc1* and/or *iro1*). Genomes with *Kp*VP-1 were detected in 55 unique sublineages including hypervirulence associated lineages (n = 745 genomes) but also known MDR lineages (n = 2323). Indeed, the majority of genomes from known hypervirulence-associated sublineages SL23 and SL86 (associated with K1 and K2 capsular serotypes, respectively) were found to typically carry both *iuc* and *iro* loci (93% of SL23, 83% of SL86; see Fig. 5a), supporting the notion that the ability to utilise both siderophores facilitates persistence and virulence. On the contrary, most MDR strains harbour only *iuc* (n = 2230; 96%), with a small number carrying both loci (n = 84; 3.6%). Relatively few genomes carried *iro1* only (n = 61 genomes across 9 sublineages); demonstrating that *iro* is most commonly co-inherited with *iuc*.

Interestingly, strains that were isolated from human faecal or rectal samples mostly harboured only *iuc* (n = 259/303; see Fig. 5b), with a lower number carrying both (n = 43) or only *iro* loci (n = 1). This corroborates our findings in Fig. 4 showing that aerobactin is primarily providing SGH10 with an advantage in gut colonisation. Isolates from human blood, liver, and respiratory samples mostly harboured either *iuc* alone or both loci (99%, 95%, and 99%, respectively), suggesting both siderophores may be important in systemic infection (Fig. 5). While we demonstrate that salmochelin is important in extra-intestinal infection in mice, under a very low dose and less acute infection, aerobactin also seems to contribute to virulence although to a lesser extent than salmochelin (Fig. 3d). In essence, the *iro* loci is most often co-inherited together with *iuc*, suggesting that the carriage of both siderophores confer an evolutionary

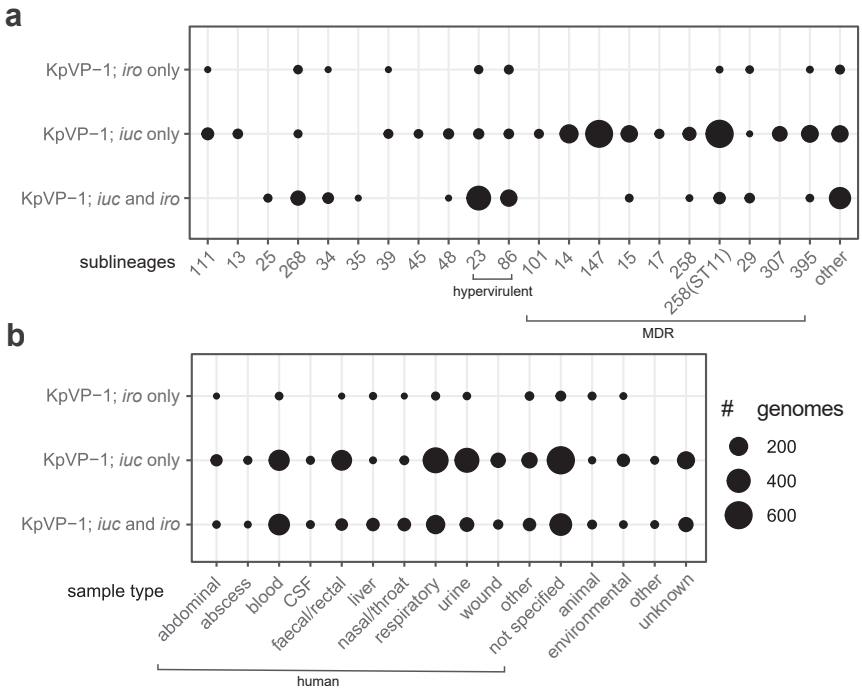

***Fig. 5: Iro* and *iuc* loci are commonly co-inherited in *Kp*VP-1 harbouring hypervirulent *Kp* strains**. Presence and absence of *iuc1* and *iro1* in 3928 *Klebsiella pneumoniae* genomes with the *Kp*VP-1 virulence plasmid, categorised by **a)** sublineages and **b)** sample type or source. Sublineages are defined on the basis of the 629-loci cgMLST scheme and associated cgLIN code nomenclature. The size of the circles correspond to genome counts corresponding to each category. Hypervirulent and MDR sublineages, and samples sourced from patients/humans are indicated.

advantage, especially in the context of perpetuating human disease.

Discussion

Our study utilised SGH10, a hypervirulent canonical ST23 K1 strain because this lineage causes the majority of liver abscesses in Asia,[9] and provides one of the few reports on key virulence determinants harboured on the *Kp*VP in relation to pathogenicity *in vivo*. The pathogenesis of hv*Kp* is known to first involve host intestinal colonisation, where it may translocate to the liver via the hepatic portal vein and then disseminate to establish metastatic infections at distal sites such as the lungs, brain, and eyes. Therefore, it should not be assumed that the key virulence factors harboured on the *Kp*VP (*iuc*, *rmpA,* and *iro*) would play the same role in each organ niche. Although the primary siderophores produced by SGH10 are aerobactin and enterobactin *in vitro*, our study demonstrates that aerobactin and enterobactin-derived salmochelin do not necessarily offer functional redundancy in different host infection contexts.

We demonstrated that neither aerobactin nor salmochelin was crucial in promoting bacterial growth in the lungs, whereas the presence of the hypermucoviscous capsule modulated by *rmpA* was the major determinant. Interestingly, survival experiments further revealed a non-statistically significant Δ*iroB* attenuation and a slight but statistically significant Δ*iroBiucCD* attenuation for mortality, suggesting a role for the iron siderophores in the later systemic progression of the disease. We did, however, observe marginally higher CFUs of Δ*iroB* and Δ*iroBiucCD* mutants in the lungs. While the contribution of aerobactin was not examined in their study, Holden et al. previously demonstrated that the release of siderophores such as enterobactin, salmochelin, and yersiniabactin themselves can trigger the production of proinflammatory cytokines such as IL-6 and CXCL-1, CXCL-2 during lung infection.[30] Hence, it is possible that deletion of salmochelin may dampen immune clearance and result in higher bacterial burden.

Russo et al. recently proposed that LD_{50} data generated from subcutaneous infection with strains of different hv*Kp* ST lineages harbouring deletion of the entire virulence plasmid or its individual virulence genes could guide countermeasure development against these strains.[12] Their study clearly demonstrated the importance of the virulence plasmid to systemic virulence in all four different STs of hv*Kp*. However, the contribution of aerobactin and chromosomal factors such as yersiniabactin varied significantly across the isolates and did not demonstrate a clear and predictable pattern. It is interesting that aerobactin is found to be unimportant for systemic virulence in the canonical ST23 K1 strain and K20 isolate but is a major contributor to virulence in the K2 and several other isolates examined.[12] We similarly found that deletion of aerobactin in our K1 strain SGH10 had no significant impact on virulence in systemic infection. However, loss of *iroB* led to a significant attenuation. Since enterobactin is significantly produced by SGH10 *in vitro*, it is likely that salmochelin is also being generated through glucosylation of enterobactin by *iroB*. Salmochelin can thus contribute to pathogenesis by evading binding by LCN-2 produced by the host to sequester unmodified enterobactin.[31] Studies in *E. coli* have found that catecholate siderophores such as enterobactin and salmochelin retain highest stability and iron chelating ability at neutral to alkaline pH whereas aerobactin is most stable and active at acidic pH.[20] It is possible that during systemic infection, the blood and tissue organs are at neutral or slightly alkaline pH, favouring the action of salmochelin over aerobactin. Furthermore, studies in *Salmonella enterica* demonstrated that salmochelin was superior in facilitating iron uptake compared to enterobactin in the presence of serum albumin, likely due to reduced binding to albumin that inhibits siderophore uptake.[32] To confirm whether the decreased virulence of the Δ*iroB* mutant was due to the inability to use salmochelin to acquire iron rather than other properties of salmochelin on the host, we show that the deletion of the salmochelin receptor *iroN* also leads to attenuation *in vivo*. While the *iroN* mutant had marginally lower hypermucoviscosity than wild type, it is unlikely to be significant enough to attenuate virulence to the extent we observed. In an earlier study by Russo et al., deletion of salmochelin had no effect on survival in both subcutaneous and pulmonary infection models whereas aerobactin played a key role,[21] while their latest study did not examine salmochelin. The differences in contribution of salmochelin and aerobactin between different lineages is intriguing. There is the possibility that the salmochelin cluster in those isolates e.g., K2 strains contain mutations or gene regulatory differences, thereby rendering salmochelin defective or less effective. Another possibility is that other factors could erode the advantage of salmochelin in these isolates due to difference in genetic context of the strains.

Conversely, we discovered that aerobactin was crucial in enabling stable gut colonisation when SGH10 was pitted against recovering commensal microbiota in capturing necessary iron for growth. As mentioned, environmental conditions can differentially affect the production of siderophores, where acidic conditions promote aerobactin production, while neutral to alkaline conditions may favour enterobactin and salmochelin production and facilitate higher binding affinity to ferric ion.[20,33] This could potentially account for the opposing requirements for salmochelin and aerobactin in systemic infection and gut colonisation models respectively, since the peritoneal environment in humans

appears to be neutral to alkaline,[34] while the caecal to colonic pH has been reported to be between pH 4.5 and 6 in mice and pH 5.7–7 in humans.[35] In this study, we narrowed down the region on the virulence plasmid to the stretch encompassing *iuc, rmpA, and iro* (~37 kb) that appears solely responsible for virulence contributed by the plasmid. Thus, acquiring the *iuc-rmp-iro* region may allow SGH10 to effectively adapt its iron acquisition strategies to varying environmental conditions to enhance its virulence or compete against other microbes.

The role of capsule and hypermucoviscosity in bacterial pathogenesis have been extensively investigated in several studies, where they form a substantial barrier against complement opsonisation and direct immune capture by phagocytes.[13,36,37] *rmpA* regulates the synthesis of capsular polysaccharide and its deletion leads to a drastic loss in mucoviscosity, therefore, it is not surprising that *rmpA* is crucial to immune evasion in systemic and pulmonary infections. We identified *rmpA* as the most important determinant of virulence during acute intranasal infection in the lung pneumonia model, and during systemic infection. Even so, in systemic infection, single deletions of *rmpA* or *iroB* did not result in a complete attenuation in mortality at higher infection doses, but the deletion of the region encompassing *iuc*, *rmp*, and *iro* did. Therefore, the rate of bacterial growth that hinges upon iron acquisition and the ability of the immune response to clear the pathogen, could both dictate the eventual outcome of infection.

While *Kp*VP evidently provides *Kp* with an arsenal of critical virulence determinants, the bacteria also bear the fitness cost of carrying such a large plasmid. During *in vitro* evolution, we found that in SGH10, *Kp*VP is lost completely or carries deletions in the siderophore genes in almost 50% of the strains (Supp Fig S4). In our gut colonisation model, the isogenic plasmid-null mutant showed a fitness advantage over the wild-type. Thus, it is clear that the plasmid exerts a significant fitness cost and can be lost in the absence of selection pressure. In the gut colonisation model, the loss of the 37 kb *iuc-rmp-iro* region resulted in a less severe drop in colonisation load compared to either or both the siderophore mutants, as well as the *rmpA* mutant. One would expect deletion of the entire *iuc-rmp-iro* region to show the biggest decrease in colonisation due to the additive effects of losing three loci that contribute to decrease in colonisation. However, there is a balance between the fitness cost of producing each virulence factor, and the selection pressure for maintaining that factor for optimal survival. Perhaps deletion of the 37 kb region provided a substantial reduction in the cost of maintaining these three systems such that overall, the metabolic gain outweighs the inability to produce these factors. Another possibility is that the extensive region contains other genes that contribute to fitness cost. We believe this balance between fitness cost versus carrying a hypermucoid capsule is also at play in our gut colonisation data, where the capsule null mutant colonised just as well as the wildtype bacteria, but the *rmpA* mutant colonised poorer. This seems to indicate that the hypermucoid capsule contributes to better colonisation particularly from day 5 onwards where the endogenous microbiota is recovering in the antibiotic treated mice. Yet if the entire capsule is lost such as in the capsule-null mutant, the additional fitness advantage of not producing a capsule could compensate for not having the hypermucoid capsule.

Therefore, this study emphasises that the importance of each virulence factor depends on the infection context, and it is difficult to generalise using one model, particularly since hv*Kp* can cause disease in various manifestations and niches. It also means that should one of these virulence factors be lost, it may constrain the isolate to a particular niche. For instance, if *iuc* plays an outsized role during gut colonisation, one may expect to see strains that have lost *iro* to be confined more to the gut and are less able to spread systemically. In fact, one example is seen in capsule loss mutants that were indeed found to be confined in the urinary tract.[38]

It is interesting to see the close association of the three major virulence determinants (*iuc-rmp-iro*) co-located next to each other on the virulence plasmid. Each confers virulence and fitness advantage to the bacterium in different host infection contexts, and there could be a strong evolutionary selection for them to be retained in the life cycles of the hypervirulent lineages. We had previously discovered *iroP*, a negative regulator of the Type 3 fimbriae encoded within the salmochelin cluster,[10] showing another example of how these plasmid virulence genes interact with host chromosomal genes and influence each other, apart from the example of *rmpA* regulating the capsule operon. The evolutionary trajectory of each genetic element associated with its bacterial host requires balancing between acquiring virulence and incurring fitness costs.

It is also intriguing that the different STs used by Russo et al. all contained the *Kp*VP-1 plasmid with the same *iuc1* and *iro1* variants, yet the requirements of the genetic elements such as aerobactin differs.[12] The limitations of our study include only studying the ST23 K1 strain. Future work examining other STs with different K types would be important, particularly for the role of salmochelin. We also do not yet understand whether siderophores are differentially regulated in various niches, and whether iron availability at different host niches may differentially impact their contribution to virulence.

However, our study reveals that the differential importance of iron siderophores and the *rmpA* regulator on the virulence plasmid to bacterial virulence is niche specific. Therefore, in contemplating what factors to

focus on when targeting hv*Kp*, we should also consider how these plasmid operons could be encoding regulators that interact with and modulate chromosomally encoded factors to further fine-tune its pathogenesis and survival within the complex infection niches. Furthermore, the integration of the plasmid operons with host chromosomal networks may undergo a period of adaptation and selection, and this process could differ between the lineages due to a difference in evolutionary history.

Contributors

CL designed and performed experiments, analysed data and co-wrote the original draft.

CYZ created genetic mutants, performed experiments and analysed data.

GC, WHWC, MY, and KYEL performed experiments, YC created genetic mutants.

THT performed experiments and analysed data.

MMCL curated data and performed formal analysis.

YHG conceptualised the study, analysed data, co-wrote the original draft, acquired funding, provided overall administration and supervision of the project.

CL and YHG have verified the underlying data.

All authors have read and approved the final version of the manuscript.

Data sharing statement

All the data are contained within the manuscript and Supplementary Information.

Declaration of interests

The authors declare no conflicts of interest.

Acknowledgements

This work was supported by grants from National Research Foundation (MOH-000925-00) to YHG and OFYIRG22jul-0042 by the National Medical Research Council (NMRC) to THT.

Appendix A. Supplementary data

Supplementary data related to this article can be found at https://doi.org/10.1016/j.ebiom.2025.105683.

References

1 Murray CJL. The global burden of disease study at 30 years. *Nat Med*. 2022;28(10):2019–2026.
2 Zhang R, Lin D, Chan EW, Gu D, Chen GX, Chen S. Emergence of carbapenem-resistant serotype K1 hypervirulent Klebsiella pneumoniae strains in China. *Antimicrob Agents Chemother*. 2016;60(1):709–711.
3 Fu Y, Xu M, Liu Y, Li A, Zhou J. Virulence and genomic features of a bla (CTX-M-3) and bla (CTX-M-14) coharboring hypermucoviscous Klebsiella pneumoniae of serotype K2 and ST65. *Infect Drug Resist*. 2019;12:145–159.
4 Li P, Liang Q, Liu W, et al. Convergence of carbapenem resistance and hypervirulence in a highly-transmissible ST11 clone of K. pneumoniae: an epidemiological, genomic and functional study. *Virulence*. 2021;12(1):377–388.
5 Nagaraj G, Shamanna V, Govindan V, et al. High-resolution genomic profiling of carbapenem-resistant Klebsiella pneumoniae isolates: a multicentric retrospective Indian study. *Clin Infect Dis*. 2021;73(Suppl_4):S300–S307.
6 Fung CP, Lin YT, Lin JC, et al. Klebsiella pneumoniae in gastrointestinal tract and pyogenic liver abscess. *Emerg Infect Dis*. 2012;18(8):1322–1325.
7 Choby JE, Howard-Anderson J, Weiss DS. Hypervirulent Klebsiella pneumoniae - clinical and molecular perspectives. *J Intern Med*. 2020;287(3):283–300.
8 Nguyen Q, Nguyen YTP, Ha TT, et al. Genomic insights unveil the plasmid transfer mechanism and epidemiology of hypervirulent Klebsiella pneumoniae in Vietnam. *Nat Commun*. 2024;15(1):4187.
9 Lam MMC, Wyres KL, Duchene S, et al. Population genomics of hypervirulent Klebsiella pneumoniae clonal-group 23 reveals early emergence and rapid global dissemination. *Nat Commun*. 2018;9(1):2703.
10 Chu WHW, Tan YH, Tan SY, et al. Acquisition of regulator on virulence plasmid of hypervirulent Klebsiella allows bacterial lifestyle switch in response to iron. *mBio*. 2023;14(4):e0129723.
11 Nassif X, Sansonetti PJ. Correlation of the virulence of Klebsiella pneumoniae K1 and K2 with the presence of a plasmid encoding aerobactin. *Infect Immun*. 1986;54(3):603–608.
12 Russo TA, Carlino-MacDonald U, Drayer ZJ, et al. Deciphering the relative importance of genetic elements in hypervirulent Klebsiella pneumoniae to guide countermeasure development. *eBioMedicine*. 2024;107:105302.
13 Tan YH, Chen Y, Chu WHW, Sham LT, Gan YH. Cell envelope defects of different capsule-null mutants in K1 hypervirulent Klebsiella pneumoniae can affect bacterial pathogenesis. *Mol Microbiol*. 2020;113(5):889–905.
14 Lee IR, Molton JS, Wyres KL, et al. Differential host susceptibility and bacterial virulence factors driving *Klebsiella* liver abscess in an ethnically diverse population. *Sci Rep*. 2016;6(1):29316.
15 Arora NK, Verma M. Modified microplate method for rapid and efficient estimation of siderophore produced by bacteria. *3 Biotech*. 2017;7(6):381.
16 Teo T-H, Ayuni NN, Yin M, et al. Differential mucosal tropism and dissemination of classical and hypervirulent Klebsiella pneumoniae infection. *iScience*. 2024;27(2):108875.
17 Argimón S, David S, Underwood A, et al. Rapid genomic characterization and global surveillance of Klebsiella using pathogenwatch. *Clin Infect Dis*. 2021;73(Suppl_4):S325–s335.
18 Lam MMC, Wick RR, Watts SC, Cerdeira LT, Wyres KL, Holt KE. A genomic surveillance framework and genotyping tool for Klebsiella pneumoniae and its related species complex. *Nat Commun*. 2021;12(1):4188.
19 Hennart M, Guglielmini J, Bridel S, et al. A dual barcoding approach to bacterial strain nomenclature: genomic taxonomy of Klebsiella pneumoniae strains. *Mol Biol Evol*. 2022;39(7):msac135.
20 Valdebenito M, Crumbliss AL, Winkelmann G, Hantke K. Environmental factors influence the production of enterobactin, salmochelin, aerobactin, and yersiniabactin in Escherichia coli strain Nissle 1917. *Int J Med Microbiol*. 2006;296(8):513–520.
21 Russo TA, Olson R, MacDonald U, Beanan J, Davidson BA. Aerobactin, but not yersiniabactin, salmochelin, or enterobactin, enables the growth/survival of hypervirulent (hypermucoviscous) Klebsiella pneumoniae ex vivo and in vivo. *Infect Immun*. 2015;83(8):3325–3333.
22 Fischbach MA, Lin H, Liu DR, Walsh CT. In vitro characterization of IroB, a pathogen-associated C-glycosyltransferase. *Proc Natl Acad Sci U S A*. 2005;102(3):571–576.
23 Lin CT, Wu CC, Chen YS, et al. Fur regulation of the capsular polysaccharide biosynthesis and iron-acquisition systems in Klebsiella pneumoniae CG43. *Microbiology (Reading)*. 2011;157(Pt 2):419–429.
24 Cheng HY, Chen YS, Wu CY, Chang HY, Lai YC, Peng HL. RmpA regulation of capsular polysaccharide biosynthesis in Klebsiella pneumoniae CG43. *J Bacteriol*. 2010;192(12):3144–3158.
25 Shon AS, Bajwa RP, Russo TA. Hypervirulent (hypermucoviscous) Klebsiella pneumoniae: a new and dangerous breed. *Virulence*. 2013;4(2):107–118.
26 Tan YH, Arros P, Berrios-Pasten C, et al. Hypervirulent Klebsiella pneumoniae employs genomic island encoded toxins against bacterial competitors in the gut. *ISME J*. 2024;18(1):wrae054.
27 Chng KR, Ghosh TS, Tan YH, et al. Metagenome-wide association analysis identifies microbial determinants of post-antibiotic ecological recovery in the gut. *Nat Ecol Evol*. 2020;4(9):1256–1267.
28 Lourenco M, Chaffringeon L, Lamy-Besnier Q, et al. The gut environment regulates bacterial gene expression which modulates susceptibility to bacteriophage infection. *Cell Host Microbe*. 2022;30(4):556–569.e5.
29 Wilson BR, Bogdan AR, Miyazawa M, Hashimoto K, Tsuji Y. Siderophores in iron metabolism: from mechanism to therapy potential. *Trends Mol Med*. 2016;22(12):1077–1090.

30 Holden VI, Breen P, Houle S, Dozois CM, Bachman MA. Klebsiella pneumoniae siderophores induce inflammation, bacterial dissemination, and HIF-1alpha stabilization during pneumonia. *mBio*. 2016;7(5):e01397-16.
31 Fischbach MA, Lin H, Zhou L, et al. The pathogen-associated iroA gene cluster mediates bacterial evasion of lipocalin 2. *Proc Natl Acad Sci U S A*. 2006;103(44):16502–16507.
32 Bister B, Bischoff D, Nicholson GJ, et al. The structure of salmochelins: C-glucosylated enterobactins of Salmonella enterica§. *Biometals*. 2004;17(4):471–481.
33 Watts RE, Totsika M, Challinor VL, et al. Contribution of siderophore systems to growth and urinary tract colonization of asymptomatic bacteriuria Escherichia coli. *Infect Immun*. 2012;80(1):333–344.
34 diZerega GS, Rodgers KE. Peritoneal fluid. In: *The Peritoneum*. New York: Springer-Verlag; 1992:26–56.
35 Woodward SE, Neufeld LMP, Pena-Diaz J, et al. Both pathogen and host dynamically adapt pH responses along the intestinal tract during enteric bacterial infection. *PLoS Biol*. 2024;22(8):e3002761.
36 Lin ZW, Zheng JX, Bai B, et al. Characteristics of hypervirulent Klebsiella pneumoniae: does low expression of rmpA contribute to the absence of hypervirulence? *Front Microbiol*. 2020;11:436.
37 Xu Q, Yang X, Chan EWC, Chen S. The hypermucoviscosity of hypervirulent K. pneumoniae confers the ability to evade neutrophil-mediated phagocytosis. *Virulence*. 2021;12(1):2050–2059.
38 Ernst CM, Braxton JR, Rodriguez-Osorio CA, et al. Adaptive evolution of virulence and persistence in carbapenem-resistant Klebsiella pneumoniae. *Nat Med*. 2020;26(5):705–711.